Experimental analysis of the impact of ground movements on surface structure

Boramy Hor, Matthieu Caudron, Marwan Al Heib

Experimental analysis of the impact of ground movements on surface structure

B. Hor[1,2], M. Caudron[1] & M. Al Heib[1]
[1]INERIS, Parc technologique Alata, 60550 Verneuil en Halatte, France
[2]Université de Lyon, INSA-Lyon, LGCIE, 69621 Villeurbanne, France
F. Emeriault
Grenoble-INP, UJF-Grenoble 1, CNRS UMR 5521, 3SR, Grenoble F-38041, France

ABSTRACT
Man's activity frequently causes ground movements: the most notable examples of ground movements are provided by the mining industry in the form of subsidence. Consequently, mining subsidence can damage the surface structures. Many empirical approaches have been developed to predict structure damage using ground movements measured in greenfield conditions by assuming that the presence of a building has no effect on the settlement prediction. To improve our understanding of that effect and investigate the potential damage to the building, we have undertaken an experimental research program by means of a large three-dimensional physical model designed to simulate mining-induced ground movements. The results pointed out the effect of building structure on greenfield movements to be taken into account and enabled an analysis of the damage to the surface building, based on the existing damage estimation approaches.

RÉSUMÉ
L'activité humaine cause fréquemment des mouvements de terrain. Les mouvements de terrain sous la forme d'affaissement sont induits par l'exploitation minière. Les affaissements miniers peuvent endommager les structures en surface. Des approches empiriques ont été développées pour prévoir les dommages au bâti en utilisant les caractéristiques des mouvements de terrain sans prendre en compte l'effet de la présence des constructions en surface. Afin d'étudier ces effets et d'investiguer les dommages potentiels sur le bâti, nous avons réalisé une étude expérimentale à l'aide d'un modèle réduit tridimensionnel de grandes dimensions permettant de simuler des mouvements de terrain dus aux mines. Les résultats expérimentaux montrent l'influence de la présence du bâti sur les mouvements du sol, qui doit être prise en compte dans l'estimation de dommage, et permettent d'apprécier la prévision des dégradations de la structure bâtie basée sur les méthodes existantes.

1 INTRODUCTION

Subsidence of the ground surface can be regarded as ground movement which takes place due to the extraction of mineral resources. It is an inevitable consequence of mining activities and reflects the movements which occur in the mined out area. Unfortunately, subsidence can and does have serious effects on surface structures and services. Prior to construction, the ground movements should be predicted and their consequences on the structures and services should be assessed. Many research projects have been focused on the prediction of structure damage prediction by applying empirical (NCB 1975; Wagner & Schümann 1991) or analytical approaches (Burland & Wroth 1974; Boscardin & Cording 1989; Burland 1995). Yet, these approaches present an important limitation, since they are usually based on greenfield predictions without taking the influence of building stiffness or soil-structure interaction into account. Research using numerical analysis has allowed the effect of building stiffness on greenfield movements to be taken into account (Potts & Addenbrooke 1997). However, there is still great uncertainty about how to estimate the building stiffness itself and how to assess the soil-structure effects. Standing & Burland (2008) and Dimmock & Mair (2008) have provided some evidence of the effect of building stiffness and soil-structure interaction on settlement prediction for tunnelling based on observation data. Standing & Burland (2008), on the other hand, suggested that the methodology for categorising and assessing damage (according to Burland 1995) and incorporating building stiffness into the prediction of building deformations (according to Potts & Addenbrooke 1997) developed for tunneling-induced ground movements could be applied for cases involving mining–induced subsidence if the greenfield movements can be predicted reliably.

The aim of our research is to use an experimental modeling approach by means of a large 3D physical model developed by "Institut National de l'Environnement industriel et des Risques (INERIS)". The model makes it possible to represent a variety of ground movement geometries, and then to study the impact of ground subsidence due to mining on surface buildings by taking soil-structure interaction into account. Another objective is to evaluate the building damage based on the existing approaches.

This paper first briefly outlines the characteristics of mining-induced subsidence and its consequences on the surface structure, and then summarises the damage estimation methods for buildings located in the mining

subsidence area. An important development to predict ground movements by taking the stiffness of a building into account (Potts and Addenbrooke, 1997) will be also briefly presented. We will then give a presentation of the physical model and the building model representing an individual house. Much of the content of this paper is drawn from the discussion on the effect of soil-structure interaction and the estimation of building damage using data from experimental tests.

2 MINING SUBSIDENCE AND STRUCTURE DAMAGE

The subsidence parameters from underground excavation that are used to assess the impacts of subsidence on building structures are shown in Figure 1. When the ground movement occurs, the overlying buildings or structures are in general affected by the vertical and horizontal displacements.

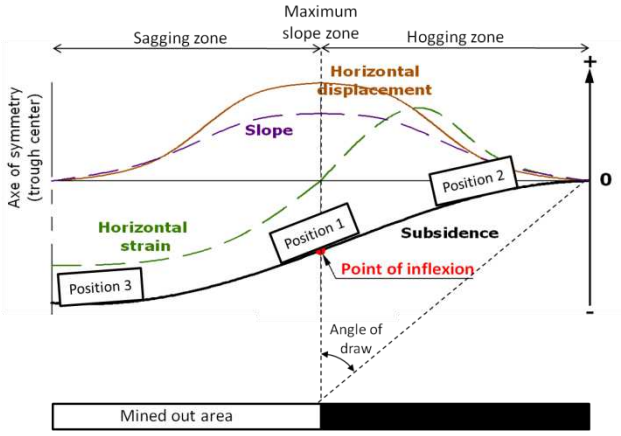

Figure 1. Subsidence parameters and structure's behaviour for different positions at ground level

Vertical displacement (S_v) due to mining generally results in a "subsidence trough." The maximum subsidence ($S_{v,max}$) is typically found around the trough center and the extent of the trough is limited by the angle of draw. The impact of subsidence on the building results from the occurrence of differential subsidence. The differential vertical movements give rise to ground slope (α).

Horizontal displacements (S_h) due to mining subsidence occur in such a way that points on the surface generally move towards the centre of the subsidence trough. Differential horizontal displacements give rise to horizontal strains (ε_h).

Ground strain is one of the major causes of impact to structures. Another major cause is curvature resulting from differential slope. Within the subsidence trough, convex or hogging curvature is accompanied by tensile strain (ε_{ht}) and concave or sagging curvature is accompanied by compressive strain (ε_{hc}). The hogging zone is separated from the sagging zone by the inflexion point where the maximum ground slope (α_{max}) and maximum horizontal displacement ($S_{h,max}$)- take place. Both tensile and compressive strains can cause cracking in a building structure, but tensile strains are more difficult to accommodate since almost all components of a structure are weaker in tension than in compression.

The transfer of ground strains into the structure occurs through friction on the underside of the foundations and ground pressure on the sides of the foundations or on buried walls. The transfer is thus dependent upon the configuration and type of foundation and its orientation to the subsidence trough. The transfer of strain is also dependent upon the types of soil that are immediately below the foundation.

3 BUILDING DAMAGE ESTIMATION

Clearly, if an estimation of the building damage due to ground movement is to be made, the classification of damage is a key issue.

3.1 Classification of damage

Many studies have been largely carried out in the UK to classify the building damage subjected to tunnelling-induced ground movements (according to Standing & Burland 2008). Three broad categories of building damage can be defined: (a) visual appearance or aesthetics, (b) serviceability or function, and (c) stability. As foundation movements increase, damage to a building will progress successively from (a) to (c).

Burland & Wroth (1974) divided these broad categories in six categories of damages, numbered from 0 to 5 in increasing severity (negligible to very severe damage). Normally categories 0, 1 and 2 relate to aesthetic damage, 3 and 4 relate to serviceability damage and 5 represents damage affecting stability.

3.2 Damage estimation methods

The damage criterion used in the above-mentioned classification system is based on the ease of repair of the visible damage (e.g. crack width of the brick or masonry structure). This damage criterion could be expressed in terms of the limiting tensile strain (ε_{lim}) developed by Burland & Wroth (1974). Boscardin & Cording (1989) went on to analyze this concept and finally showed that the categories of damage could be broadly related to ranges of ε_{lim} as presented in Table 1.

The most used method established by the UK National Coal Board (NCB 1975) makes it possible to estimate building damage as a function of the structure length and the horizontal ground strain. This method assumes that the building has no effect on the settlement prediction and the damage parameters are calculated using the predicted greenfield movements. The NCB's approach has been proposed for very long structures. In the case of individual house considered in the present analysis, the NCB's approach is useless, since it is too imprecise. Therefore, Wagner & Shümann (1991) developed another chart using the same damage parameters and based on structure damage observed mostly in South Africa. This chart, presented in Figure 2, conforms to NCB's for lengths of structure longer than 45 m.

As mentioned above, following the concept of limiting tensile strain established by Burland & Wroth (1974), Burland (1995) showed how, by combining the deflection ratio (Δ/L where Δ is the deflection over the structure length L) with the horizontal strain simple interaction diagrams relating $(\Delta/L)/\varepsilon_{lim}$ to $\varepsilon_h/\varepsilon_{lim}$ for various values of L/H could be developed. Figure 3 shows one such diagram for the case of an isotropic beam with L/H = 1 undergoing hogging. The limiting tensile strains have been converted into the associated categories of damage given by Table 1.

Table 1. Relationship between category of damage and limiting tensile strain (after Boscardin & Cording 1989)

Damage category	Normal degree of severity	Limiting tensile strain - ε_{lim} (%)
0	Negligible	0 – 0.05
1	Very slight	0.05 – 0.075
2	Slight	0.075 – 0.15
3	Moderate[1]	0.15 – 0.3
4 to 5	Severe to very severe	> 0.3

[1]Boscardin & Cording (1989) describe the damage corresponding to ε_{lim} in the range 0.15 - 0.3% as moderate to severe. However, none of the cases quoted by them exhibit severe damage for this range of strains. There is therefore no evidence to suggest that tensile strains up to 0.3% will result in severe damage.

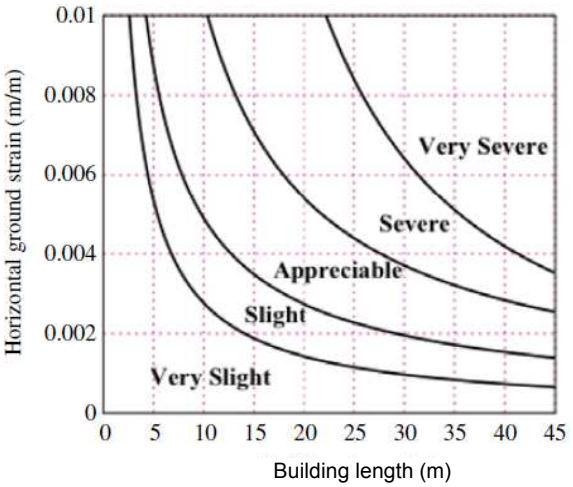

Figure 2. Damage estimation according to Wagner & Shümann (1991)

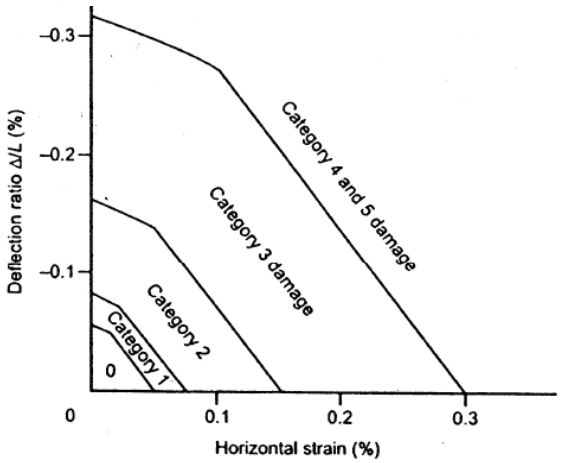

Figure 3. Damage estimation according to Burland (1995)

3.3 Influence of building stiffness on settlement prediction

The prediction of ground movements due to tunnelling and mining is normally done using empirical relationships which are based on measurements from greenfield conditions. The presence of a building is assumed to have no effect on the settlement prediction and any damage parameters are calculated using the predicted greenfield movements. This is clearly an over-simplification of reality as the stiffness of the building affects its deformation.

The Potts and Addenbrooke (1997) method addresses the influence of a surface structure on the ground movements due to tunnelling and has proved to be a useful tool in the prediction of potential building damage. A series of 2D numerical analyses of tunnel construction in greenfield conditions and beneath surface beams of varying linear elastic stiffness, oriented transverse to the tunnel, were performed to assess the difference between greenfield ground movements and those modified by the structure. The building deformation parameters of the deflection ratio and horizontal strain were expressed as a fraction of those obtained for greenfield conditions. The modification factors are defined separately for deflection ratios in sagging and hogging (see Figure 4), and for horizontal strain in compression or tension, and are as follows:

$$M^{DR_{sag}} = \frac{DR_{sag}}{DR^{g}_{sag}};\quad M^{DR_{hog}} = \frac{DR_{hog}}{DR^{g}_{hog}} \qquad [1,2]$$

$$M^{\varepsilon_{hc}} = \frac{\varepsilon_{hc}}{\varepsilon^{g}_{hc}};\quad M^{\varepsilon_{ht}} = \frac{\varepsilon_{ht}}{\varepsilon^{g}_{ht}} \qquad [3,4]$$

A design approach for predicting building deformation was proposed, which is based on factors of relative structure-soil stiffness. The relative bending stiffness, ρ* and relative axial stiffness, α*, are defined as follows:

$$\rho^* = \frac{16EI}{E_s B^4};\quad \alpha^* = \frac{2EA}{E_s B} \qquad [5,6]$$

where B is the building width, E_s is a representative soil stiffness, and E, A and I are an equivalent Young's modulus, cross-sectional area and moment of inertia for the beam. It should be noted that ρ* is not dimensionless, but rather has the dimensions m^{-1} in plane strain; this is discussed by Franzius et al. (2006) who proposed a revised dimensionless form for ρ*.

Based on the numerical analyses for 5-storey, 3-storey and 1-storey buildings and for a single slab, Potts and Addenbrooke presented a series of upper bound design curves for the variation of modification factor with relative bending stiffness and relative axial stiffness, each curve representing a different eccentricity ratio (e/B) (see Figure 5). A modification factor of 1 or greater represents fully flexible behaviour, because the building follows the greenfield settlement profile, whereas a modification factor close to zero represents very stiff behaviour (the deflection ratio of the building being almost zero).

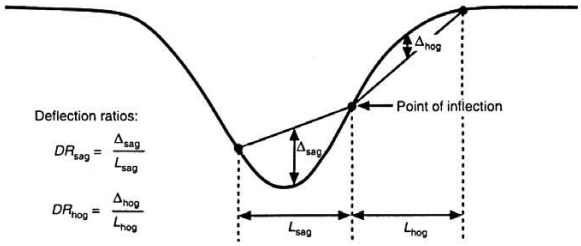

Figure 4. Definition of deflection ratios (DR) in sagging and hogging (Potts & Addenbrooke 1997)

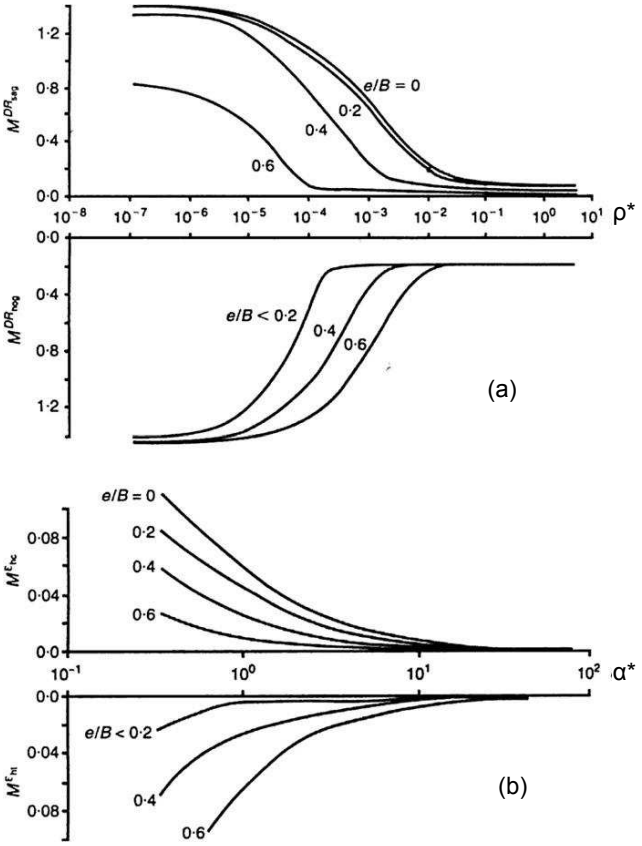

Figure 5. Design curves for modification factors for (a) deflection ratio and (b) horizontal strain (Potts & Addenbrooke, 1997)

4 THE MODELS

This paper intends to shed some light on the soil-structure interaction due to mining subsidence by means of physical modeling. To study that phenomenon we need to have a physical model that is capable of simulating the ground movements, a soil model that is a natural soil, and a building model.

4.1 The 3D physical model – simulator of ground movements

The details of the hypotheses and conception, the constraints and limitations, as well as the monitoring method of the small-scale physical model can be found in Caudron et al. (2010). The main hypothesis of the model is that it is designed to be used in a 1g (earth gravity) environment and not in a centrifuge. It is therefore difficult for quantitative interpretations of the experimental data to be made. The geometry scale factor may range up to 1/50. With a size of 2 m by 3 m in the horizontal plane for a height up to 1 m, we would be able to represent a soil block as large as 100 m by 150 m with a height of 50 m (Figure 6).

Considering underground mines as cavities to be the origin of the ground movements caused by their collapse,

the maximum depth of 50 m may appear to be an important limit to this model. However, we chose not to model the cavity itself, but only to create the subsidence trough at ground surface, which is similar to subsidence induced by mining. This is achieved by vertically moving an “electric jack” placed at the bottom (initial state) of the model downwards to the desired opening depth (final state). This mechanism for creating the subsidence trough at ground surface is presented in Figure 7.

In our study, a geometry scale factor of 1/40 with an overburden of 0.3 m and a limit subsidence extent of 1.3 m was chosen, as it provides a geometry equivalent to a real mining case. The cross-section in horizontal plane of the jack is limited to 0.25 x 0.25 m², corresponding to 10 x 10 m² at prototype scale. The selected Fontainebleau sand is very fine and clear. The diameter of the grains varies from 0.1 to 0.3 mm with D_{50} approximately 0.2 mm. A study of its mechanical properties was carried out prior to the experiments. The estimated properties of the soil mass model are presented in the Figure 7.

A measurement technique known as Digital Image Correlation (DIC) was adopted to determine the deformation of the ground and the structure at the surface in three dimensions. Two high-resolution digital cameras whose relative position is very precisely known allow plotting of the observed 3D ground and structure surfaces for each of two speckle images taken simultaneously with the left and right camera of a stereo system. Then for two different speckle images, it is possible to determine the shape, the displacement, and the strain of the specimen’s surface between different acquisition instants. In addition, this method provides an accurate result with an error smaller than 0.1 mm for a “discontinuous” surface such that of Fontainebleau sand.

4.2 The building model

A building model was created to investigate the effects of the soil-structure interactions during the formation of a subsidence trough. The geometry chosen for the building was inspired from the existing database of buildings damaged by mining subsidence in the east of France. A conventional house was considered as shown in Figure 8. This realistic but complex 3D prototype scale model was simplified for defining the small-scale model. In the first place, we considered only an elastic behavior and modeled an “equivalent slab”.

Figure 6. Overall view of the 3D physical model

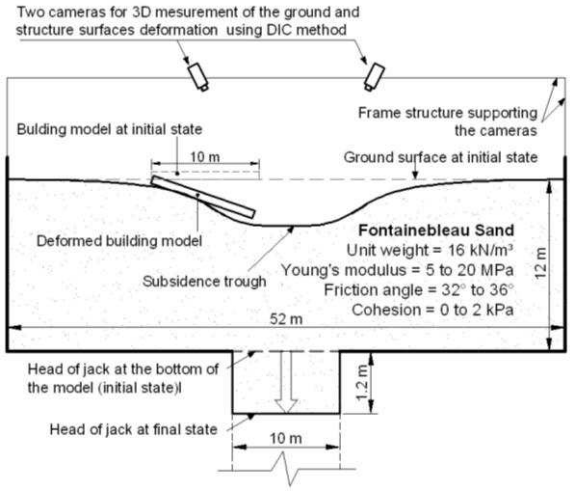

Figure 7. Vertical cross section of the 3D physical model with building model at ground surface at initial state and final state producing ground subsidence (values presented at prototype scale of 40)

The procedure to simplify an individual house to a small-scale model is successively indicated on Figure 8. Three steps were carried out for the simplification procedure.

First, the equivalent slab was determined in such a way that the bending stiffness and the axial stiffness of this slab are closely equivalent to the 3D structure. We then intentionally chose to reduce the stiffness of the slab in both directions to exacerbate the strain in the structure. Both stiffness are approximately reduced by half. The last step is to transform this very simple structure into a small scale model by respecting the factors of the scaling laws. The structure model presented in Figure 8 is indeed a U-section slab made of polycarbonate, the interior part of which is composed of lead powder in plastic bags. This allows the model to present a stiffness and a stress transmitted to the ground approximately equivalent to those of the prototype. The 5 mm width of the edge is designed to be visible to the camera for measurement during the test.

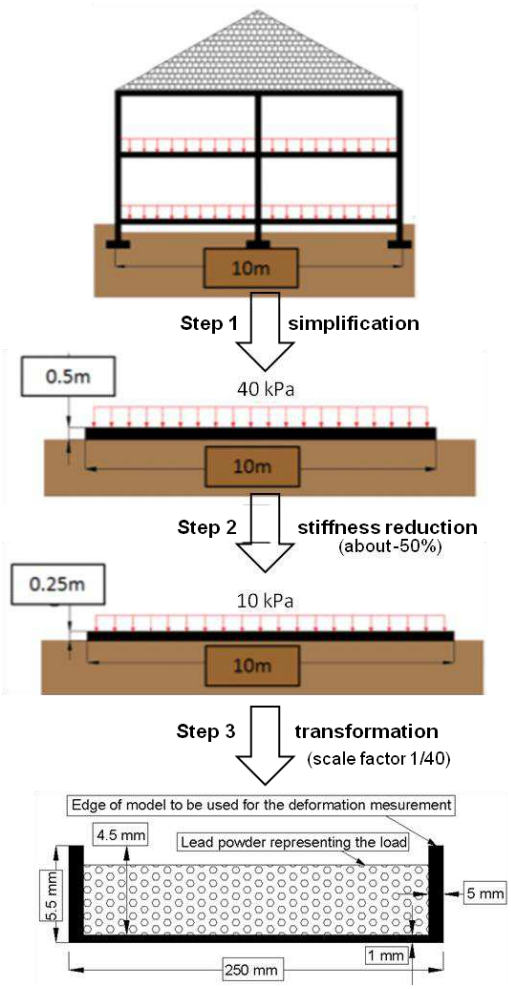

Figure 8. Simplification procedure of a 3D individual house to an equivalent small-scale slab (dimensions not to scale)

The main characteristics of the structure model and the equivalent prototype for a geometric scaling factor of 1/40 are shown in Table 2. The Table 2 also gives the value of relative bending and axial stiffness determined by equations 5 and 6 respectively.

The soil Young's modulus of 5 MPa was chosen because it corresponds to the low stress (< 1 kPa) applied on the soil below the structure. According to modification factors from the design curves of Potts & Addenbrooke (1997) as shown in Figure 5, the building model can be considered stiff for relative axial stiffness ($M^{\varepsilon hc}$ and $M^{\varepsilon ht}$ close to zero) and quite flexible for relative bending stiffness in hogging zone ($M^{DRhog} \approx 0.5$) and very flexible in sagging zone ($M^{DRhog} > 0.5$) for an eccentricity ratio e/B = 0.5 (position of structure center relevant to trough center).

To perform a test, the sand is placed manually in the physical model by layers of 0.15 m until the desired overburden height 0.3 m is reached. Each layer is compacted to obtain a certain level of density (a series of penetrometer tests was conducted to estimate the soil mass density, which is considered to be from average to dense).

Table 2. Characteristics of building model and corresponding equivalent prototype

Characteristics	Model	Scaling factor	Equivalent prototype
Width (m)	0.25	40	10
Length (m)	0.25	40	10
Total Height (m)	5.5E-3	40	0.22
Young's modulus (MPa)	2200	40	88000
Axial stiffness (MN)	0.66	40^3	42240
Bending stiffness (MN.m)	2.03E-7	40^5	20.79
Relative axial stiffness (-)	1.06	-	1.06
Relative bending stiffness (m^{-1})	1.67E-4	-	1.67E-4

After a horizontal level of the ground surface is ensured, the small-scale building model is laid directly on the ground without any foundation system. The transfer of deformation to the building model is only done by the friction between ground-building interfaces, which limits the interaction between the soil and the structure. However, this concept makes it very simple to reproduce the tests. The image acquisition by the two cameras is then started with a frequency of 0.5 Hz. The motion program of the jack is launched at the same time a first snapshot is taken by the cameras. The jack is moved downwards at a rate of 0.125 mm/s for a total displacement of 30 mm. At the end of the test, the deformations of the ground and the structure are computed by Vic3D using the DIC method. It is important to note that the building model is removed from the ground surface to capture the displacement of the soil underneath the model at the final state of the test.

5 EXPERIMENTAL RESULTS

The aim is to discuss the soil-structure interaction and the building damage estimation using the existing methods (see section 3.2). Only one position of the structure relative to the subsidence trough will be analyzed here – i.e. position 1, where the structure undergoes both compressive and tensile strains (see Figure 1). Position 1 was chosen because the structure was found to be the most affected by the ground movements (according to Caudron et al. 2010).

5.1 Greenfield ground movements

The ground movements in greenfield condition must be characterized and used as the reference for investigating the effect of soil-structure interaction.

Four identical tests were performed in order to ensure a good repeatability of the results. The variation of results from one test to another is not remarkable, but cannot be neglected. The configuration of the test is as shown in Figure 7, and the average global characteristics of the four tests are summarized in Table 3.

Table 3. Characteristics of greenfield ground movements (values at prototype scale)

Characteristics	Notation	Average value
Max. subsidence (m)	$S_{v,max}$	0.92
Max. slope (%)	α_{max}	23
Max. compressive strain (%)	$\varepsilon_{hc,max}$	-9
Max. tensile strain (%)	$\varepsilon_{ht,max}$	17
Min. of curvature radius (m)	$R_{,min}$	6.5
Distance from inflexion point to trough center (m)	i	4 to 5

5.2 Soil-structure interaction

As for the greenfield conditions, four tests were carried out for the configuration taking into account the building model. The result of one of the tests is presented in Figure 9, where the difference between the movements in greenfield and with building as well as the behaviour of the building can be seen. The results shown in Figure 9 are a slice from a 3D-surface of subsidence trough following a particular axis passing through the center of the building to that of the trough.

We can clearly see that the building causes important modifications in the soil displacement at ground level. The trough, formerly symmetrical under greenfield conditions, shows clearly some dissymmetry with the presence of the building.

Due to the load of the building and the contact with the ground, the trough size is enlarged. As a result, the ground slope is lessened. The building seems to reduce vertical ground displacement slightly. It is abnormal that the horizontal ground displacement in configuration with building is greater than that in greenfied. This could be explained by the fact that the building is located in the maximum slope area and that the ground could deform as the building model is removed to observe the subsidence trough.

The building behaviour deforms as a rigid body, since the horizontal displacement is almost a constant value along its length. Depending on the relative displacement of the ground in relation to the building model, three different zones may be distinguished.

In the center part of the trough, loss of support appears as the ground falls off the building due to a more substantial displacement. At the center part of the structure, the contact between the ground and the building is kept, and so important deformation of the building occurs, since the transfer of ground strains to the building is done by the friction from contact between the two surfaces. For the last part, the rigid body rotation of the building creates heave from the ground surface. The ground deformations in greenfield and with building, and the building deformation are compared and synthesized in Table 4.

Determining the deflection ratio of the structure is not straightforward. Two methods were then adopted to estimate the deflection ratio of the structure. First, it is determined by taking the maximum deflection (Δ) relative to the line connecting two reference points on either side (c,d) divided by the distance between the two reference points (see Figure 10). In another way, the deflection ratio of the structure is measured by the fraction of the maximum vertical distance (Δ_h) between the trough and the building model over the distance between two reference points (a,b) defining the contact zone. The range value obtained from both methods is presented in Table 4. The deflection of the ground is measured following the Potts & Addenbrooke approach (see Figure 4). The slope and strain present average values determined by differential vertical displacement and horizontal displacement respectively at the location of the building (c,d).

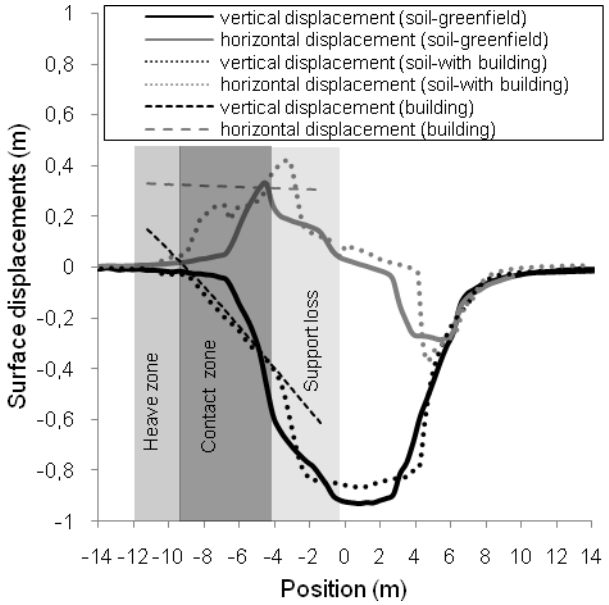

Figure 9. Displacements of the ground with and without structure at the surface and those of the structure (value at prototype scale)

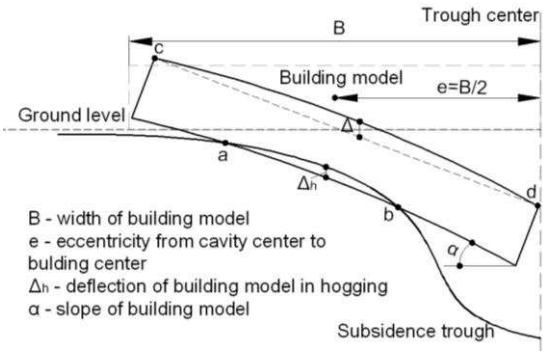

Figure 10. Building deformation within the hogging zone

It can be seen that the measured deformations of the building are relatively small compared to those of the ground. Reasons could be that the building is just laid on the ground (no foundation system), the axial stiffness of the building is relatively important, and finally the building model is designed to perform in the elastic domain.

Table 4. Comparison between the ground deformation determined in greenfield and with building, and the building deformation (values at prototype scale)

Characteristics	Green-field	With building	Building
Max. Subsidence (m)	0.92	0.91	0.55
Slope (%)	8.93	8.55	8.2
Tensile Strain (%)	3.7	4.8	0.23
Deflection ratio in hogging (%)	1.7	1.04	0.48 to 0.53

The Potts & Addenbrooke (1997) approach shows that the ground strain can transfer from 0 to 10% to the surface building (see Figure 5b). If we consider the damage estimation chart of Wagner & Shümann (1991), in which the ground strain (varies from 0 to 1%) is a damage estimation criteria, and Burland's chart (1995) based on structure strain (varies from 0 to 0.3%), we could estimate that, for a building 10 m long, the transfer from ground strain into the building is about 26%. Around 6.2% of the ground strain is transmitted to the building according to the results of physical modeling (Table 4)

The soil-structure interaction is thus clearly identified: the strains measured on the building are very different from those measured in greenfield condition, and that effect has to be taken into account for predicting building damage.

5.3 Building damage assessment

As shown in Table 5, with the data obtained from the physical model tests, the damage of the building model can be evaluated using the two-parameter charts presented in section 3.2.

The empirical chart of Wagner & Shümann (1991) (see Figure 2), which assumes that the building has no effect on the settlement prediction and the damage parameter (horizontal ground strain), is calculated using the predicted greenfield movements, makes it possible to estimate the risk level of the building model, which falls in severe to very severe damage. This is clearly an over-simplification of reality, as the stiffness of the building affects the transfer of ground strain to the surface building.

According to the analytical chart of Burland (1995) (see Figure 3) and with the movements of building models measured from the test, the likely damage of the building model is found from severe to very severe degree.

The Burland chart also makes it possible to predict the building damage from greenfield movements with the effect of building stiffness developed by Potts & Addenbrooke (1997). For each combination of the soil-structure relative bending and axial stiffness (see Table 2) and eccentricity ratio (e/B = 0.5), modification factors can be taken from the design curves of Figure 5. Then, the greenfield values of the deflection ratio and horizontal strain in hogging are multiplied by the respective modification factors (equations 2 and 4) to obtain those likely to be imposed on the structure. The combinations of hogging deflection ratio and tensile strain were then input into the Burland chart to quantify the likely building damage. This also estimates the damage of the structure from severe to very severe.

Table 5. Damage estimation of building model

	Damage parameter			
Damage estimation method	L (m)	ε_{ht} (%)	DR_{hog} (%)	Degree of damage
Wagner & Shümann (1991)	10	3.7	-	Severe to very severe
Burland (1995) using measurements[1]	10	0.23	0.48 to 0.53	Severe to very severe
Burland (1995) using Potts & Addenbrooke (1997)[2]	10	0.18	2.04	Severe to very severe

L: building length; ε_{ht}: horizontal ground or structure strain; DR_{hog}: deflection ratio of structure in hogging zone

[1] The structure deformation is obtained from measurements

[2] The structure deformation based on the ground movements in greenfield and the soil-structure interaction effect

Hence, the degree of building damage resulting from any estimation approach is from severe to very severe.

A good agreement between the building tensile strains determined from direct measurement and from greenfield movements with soil-structure interaction effect can be drawn from the Table 5. However, an important difference in building deflection ratios can be observed: about 4 times of the deflection ratio predicted from Greenfield incorporating soil-structure interaction according to Potts & Addenbrooke greater than that from the measurement. The cause could be explained by the hypothesis adopted in Potts & Addenbrooke approach that the building follows the ground movements, which is different from the behavior observed on the building model where the support loss occurs (see Figure 9). In addition, the elastic behavior of the building model can only be subjected to a maximum deflection ratio of 0.6%.

6 CONCLUSIONS AND PROSPECTS

The soil-structure interaction has been studied using 3D physical modeling making it possible to simulate the subsidence trough at the ground level. A simple structure model representing an individual house was designed to observe the importance of the soil-structure interaction to be taken into account for predicting structure deformation. The importance of building stiffness was proved by comparing the amount of strain transferred from the ground to the building obtained from experiments and from the design curves developed by Potts & Addenbrooke (1997).

The building damage has also been assessed using an empirical method applied for mining and another method used for tunneling. The latter makes it possible to

estimate the damage based on the measured structure deformation and the modified greenfield movement with soil-structure interaction effect using the Potts & Addenbrooke approach. The degree of building damage was found to be severe to very severe for the different damage estimation methods. This shows a great coherence between them. However, it should be noted that the very critical damage obtained from the Burland chart is not due to the tensile strains, but to the excessive deflection ratio. The building strain determined from the greenfield taking the building stiffness effect into consideration is close to that from the experiments.

The physical model still needs to be developed. The present state of the model provides very significant deformation of the ground surface. Hence, several jacks should be installed to increase the variety of subsidence trough geometry and amplitude that the apparatus is able to achieve. In parallel, the building model should also be improved to more closely represent a real building with a foundation system and the upper part of the structure.

REFERENCES

Boscardin, M.D. and Cording, E.G. 1989. Building response to excavation-induced settlement, *Journal of Geotechnical Engineering*, ASCE, 115(1): 1-21.

Burland, J.B. and Wroth, C.P. 1974. Settlement of buildings and associated damage. *SOA Review. Proc. Conf. Settlement of Structures*, Cambridge, Pentech Press, London, UK, 611-654.

Burland, J.B. 1995. Assessment of risk of damage to buildings due to tunneling and excavations. *Invited special lecture*, *in: Proc. 1st Int. Conf. Earthquake Geotechnical Engineering*, IS-Tokyo, 1189-1201.

Caudron, M., Hor, B., Emeriault, F. and AlHeib, M. 2010. A large 3D physical model: a tool to investigate the consequences of ground movements on the surface structure, *14th Int. Conf. on Experimental Mechanics*, EDP sciences, Poitiers, France, 6, 22001(1-8).

Dimmock, P.S. and Mair R.J. 2008. Effect of building stiffness on tunneling-induced ground movement, *Tunneling and Underground Space Technology*, 23: 438-450.

Franzius, J.N., Potts, D.M., Burland, J.B., 2006. The response of surface structures to tunnel construction, *Proc. Inst. Civ. Eng. Geotech. Eng.*, 159 (1), 3–17.

National Coal Board 1975. Subsidence Engineers Handbook. *National Coal Board Production Dept.*, U.K.

Potts, D.M. and Addenbrooke, T.I. 1997. A structure's influence on tunneling-induced ground movements. *Proc. Instn. Civil Engrs., Geotechnical Engineering*, 125 : 109-125.

Standing, J. and Burland, J.B. 2008. Impact of underground works on existing infrastructure, *Invited lecture in Post-Mining*, France, 1-39.

Wagner H., Shümann E.H.R. 1991. Surface effects of total coal-seam extraction by Underground mining methods, *Journal of the South African Institute of mining and metallurgy*, 91(7): 221-231.